182475: migmatitic gneiss, Big Red prospect

(Nornalup Zone, Albany–Fraser Orogen)

Location and sampling

Seemore (SH 51-12), Claypan (3837)
MGA Zone 51, 690500E 6649200N

Sampled on 17 August 2010

This sample was collected from diamond drillcore from hole BRDDH001, located on the Big Red prospect, at a depth of 278.2 – 278.6 m. The hole was drilled by Teck Australia Pty Ltd, and was co-funded through the Exploration Incentive Scheme. The drillhole is located on the Nullarbor Plain, approximately 17.0 km south of Fifty Mile Claypan, 38.0 km northeast of Native Willow Bore (Kananda Station), and 55.4 km west of radio mast R204 on the Rawlinna–Warburton Road (Connie Sue Highway).

Tectonic unit/relations

The sample is from drillhole BRDDH001, which intersected Precambrian basement rocks beneath the Mesozoic–Cenozoic Eucla Basin at a depth of 106.4 m; the total depth of the hole was 306.8 m. BRDDH001 was drilled to investigate a magnetic high, interpreted from detailed aeromagnetic data as a potential magnetite-bearing stratigraphic iron-formation, possibly associated with copper–gold mineralization (Tillick, 2010). This anomaly is located within the eastern Nornalup Zone of the Albany–Fraser Orogen, which contains 1800–1760 Ma metagranitic rocks similar in age to some metagranitic rocks in the Biranup Zone, overlain by metasedimentary rocks of the Arid Basin (Spaggiari et al., 2011). The Nornalup Zone is intruded by rocks of the Mesoproterozoic Recherche and Esperance Supersuites (Nelson et al., 1995).

The Precambrian rocks in BRDDH001 comprise interlayered granitic gneiss, metasedimentary gneiss (some of which is strongly magnetic, and possibly represents metamorphosed banded iron-formation), and amphibolite (see also Tillick, 2010). The present sample is a migmatitic gneiss with miilimetre- to centimetre-scale, foliation-parallel layers of dark, biotite-rich gneiss alternating with pink K-feldspar- and quartz-rich layers. A second sample of metasedimentary gneiss from this drillhole (GSWA 182473, Kirkland et al., 2012a) yielded a maximum depositional age of 1729 ± 27 Ma (1σ). The gneissic rocks are intruded by veins of pink, coarse-grained, granite pegmatite that crystallized at 1167 ± 2 Ma (GSWA 182474, Kirkland et al., 2012b).

Two additional samples at the Big Red prospect were dated from drillhole BRDDH002, located 2.1 km to the west of BRDDH001. A sample of migmatitic gneiss (GSWA 182476, Kirkland et al., 2012c) yielded a crystallization age of 1326 ± 6 Ma for the granite protolith. Garnet-bearing mafic granulite, of which GSWA 182477 (Kirkland et al., 2012d) is representative, provided a date of 1188 ± 4 Ma, interpreted as the age of metamorphism.

Petrographic description

The sample is of migmatitic gneiss, which is coarse grained, weakly gneissose, porphyroblastic, garnet-bearing, and mica-rich. The rock is composed of 40% feldspar, 25% biotite, 20% quartz, 10% garnet, 5% opaque oxide minerals, and minor chlorite, muscovite, and zircon. Coarse-grained garnet porphyroblasts are enveloped by aggregates of myrmekitic albite–quartz intergrowth, plagioclase, and perthite. Myrmekite is younger than plagioclase and commonly invades it. Myrmekite haloes around garnet grains represent metamorphic and/or metasomatic growth, rather than igneous micrographic or granophyric textures. Plagioclase (andesine, An46) forms discrete, inclusion-free, albite-twinned, subhedral crystals; biotite is commonly accompanied by iron-oxide minerals, and some grains are replaced by chlorite. Replacement of feldspar by patches of cryptocrystalline sericite and flakes of muscovite is considered evidence of hydrothermal alteration.

Zircon morphology

Zircons isolated from this sample are subhedral, generally rounded, and colourless and clear to black and opaque. The crystals are up to 300 μm long, and are equant to slightly elongate, with aspect ratios up to 3:1. In cathodoluminescence (CL) images, the crystals display idiomorphic zoning, contorted zoning, and curvilinear zoned structures. The wide range of internal structures observed, and the truncation of these structures by at least one generation of zircon rims, is consistent with the protolith of this gneiss being a sedimentary rock. A CL image of representative zircons is shown in Figure 1.

Analytical details

This sample was analysed on 22–23 June 2011, using SHRIMP-B, on 28 June 2011, using SHRIMP-A, and

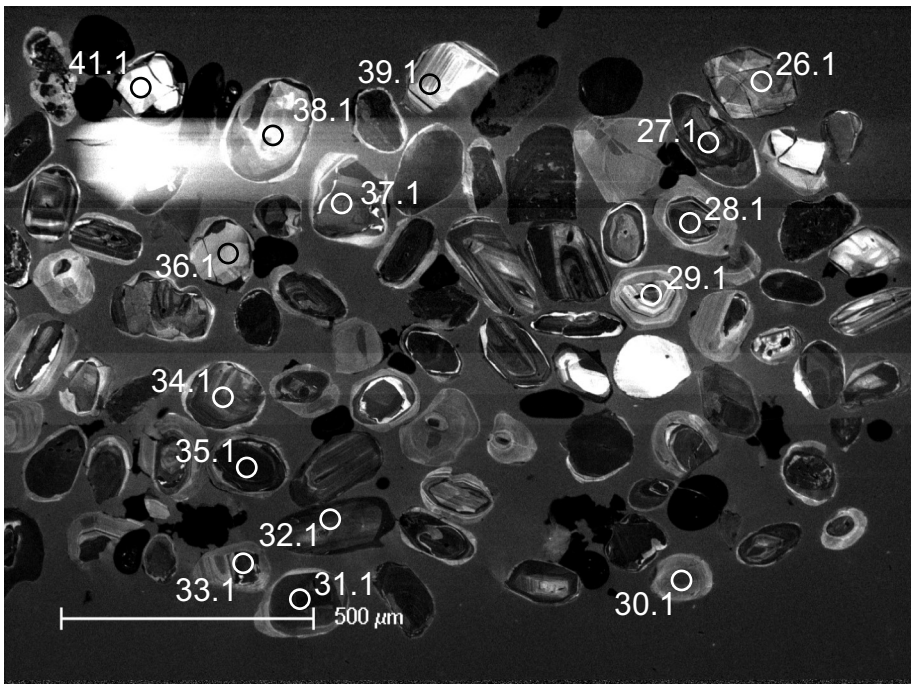

Figure 1. Cathodoluminescence image of representative zircons from sample 182475: migmatitic gneiss, Big Red prospect. Numbered circles indicate the approximate positions of analysis sites.

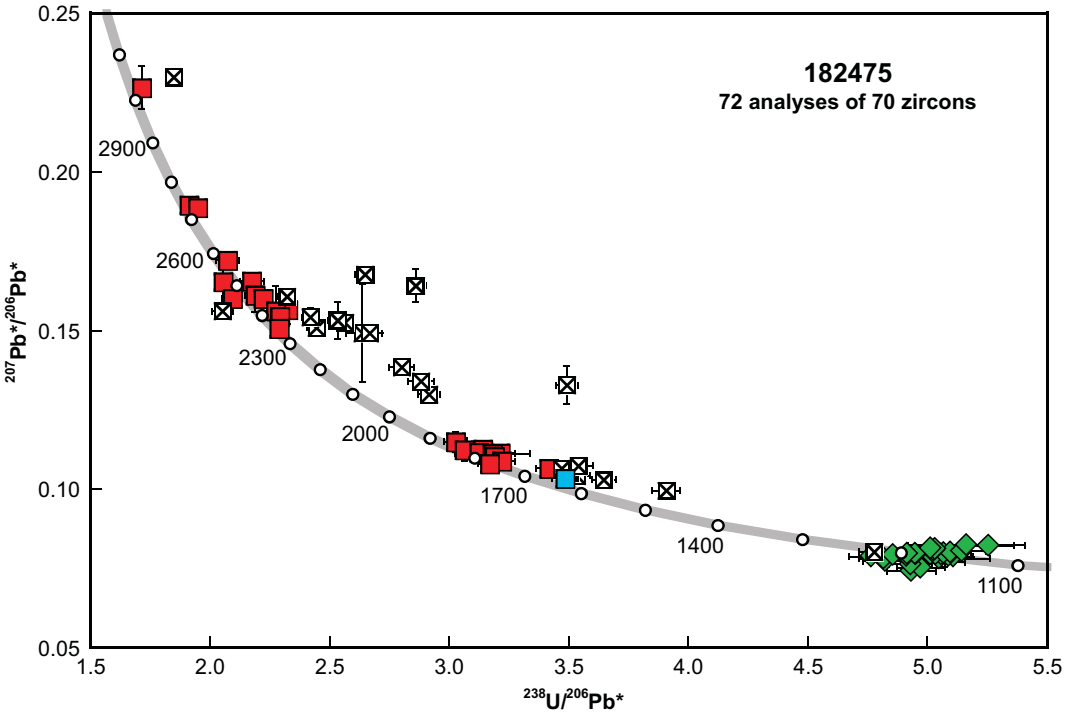

Figure 2. U–Pb analytical data for sample 182475: migmatitic gneiss, Big Red prospect. Blue square indicates Group Y (youngest detrital zircon); red squares indicate Group S (older detrital zircons); green diamonds indicate Group M (metamorphic zircon rims); crossed squares indicate Group D (date >1300 Ma and discordance >5%, or core–rim mixture).

Table 1. Ion microprobe analytical results for zircons from sample 182475: migmatitic gneiss, Big Red prospect

Group ID	Spot no.	Grain. spot	^{238}U (ppm)	^{232}Th (ppm)	$\frac{^{232}Th}{^{238}U}$	f204 (%)	$^{238}U/^{206}Pb$ ± 1σ		$^{207}Pb/^{206}Pb$ ± 1σ		$^{238}U/^{206}Pb^*$ ± 1σ		$^{207}Pb^*/^{206}Pb^*$ ± 1σ		$^{238}U/^{206}Pb^*$ date (Ma) ±1σ		$^{207}Pb^*/^{206}Pb^*$ date (Ma) ±1σ		Disc. (%)
Y	34	33.1	234	184	0.81	0.086	3.480	0.052	0.10408	0.00057	3.483	0.052	0.10333	0.00063	1627	22	1685	11	3.4
S	63	61.1	269	134	0.51	0.000	3.417	0.053	0.10652	0.00058	3.417	0.053	0.10652	0.00058	1655	23	1741	10	4.9
S	13	12.1	115	92	0.83	0.073	3.166	0.047	0.10864	0.00077	3.168	0.047	0.10801	0.00083	1768	23	1766	14	-0.1
S	30	29.1	94	146	1.60	0.000	3.219	0.055	0.10887	0.00088	3.219	0.055	0.10887	0.00088	1744	26	1781	15	2.0
S	36	35.1	142	134	0.98	0.016	3.189	0.050	0.11045	0.00072	3.189	0.050	0.11031	0.00073	1758	25	1805	12	2.6
S	64	62.1	164	61	0.38	-0.035	3.182	0.157	0.11093	0.00078	3.181	0.157	0.11124	0.00081	1762	80	1820	13	3.2
S	41	40.1	51	10	0.21	0.165	3.209	0.062	0.11276	0.00118	3.214	0.062	0.11133	0.00138	1746	30	1821	22	4.1
S	71	69.1	322	242	0.78	-0.017	3.125	0.047	0.11152	0.00054	3.125	0.047	0.11167	0.00055	1790	24	1827	9	2.0
S	8	8.1	130	58	0.46	0.030	3.062	0.044	0.11281	0.00369	3.063	0.044	0.11255	0.00370	1821	23	1841	60	1.1
S	37	36.1	153	45	0.30	0.058	3.139	0.049	0.11313	0.00070	3.141	0.049	0.11262	0.00074	1782	25	1842	12	3.3
S	56	54.1	212	44	0.21	-0.012	3.028	0.047	0.11482	0.00321	3.027	0.047	0.11493	0.00321	1840	25	1879	50	2.1
S	51	49.1	188	80	0.44	0.040	2.289	0.036	0.15100	0.00090	2.290	0.036	0.15064	0.00092	2336	31	2353	10	0.7
S	44	43.1	506	317	0.65	0.000	2.291	0.032	0.15440	0.00259	2.291	0.032	0.15440	0.00259	2335	28	2395	29	2.5
S	53	51.1	181	89	0.51	0.009	2.274	0.036	0.15627	0.00794	2.274	0.036	0.15619	0.00794	2350	32	2415	86	2.7
S	45	44.1	171	77	0.47	-0.016	2.325	0.036	0.15649	0.00443	2.324	0.036	0.15664	0.00443	2307	30	2420	48	4.7
S	40	39.1	46	49	1.11	0.115	2.091	0.042	0.16111	0.00129	2.094	0.042	0.16008	0.00139	2517	43	2457	15	-2.5
S	67	65.1	190	119	0.65	0.018	2.221	0.035	0.16034	0.00088	2.222	0.035	0.16018	0.00089	2396	32	2458	9	2.5
S	39	38.1	60	70	1.20	0.086	2.185	0.040	0.16200	0.00552	2.187	0.040	0.16123	0.00554	2428	38	2469	58	1.7
S	2	2.1	104	43	0.43	0.111	2.054	0.032	0.16633	0.00908	2.056	0.032	0.16534	0.00910	2555	33	2511	93	-1.7
S	49	47.1	39	29	0.77	0.133	2.172	0.051	0.16678	0.00204	2.175	0.051	0.16559	0.00215	2439	48	2514	22	3.0
S	42	41.1	33	26	0.83	-0.042	2.076	0.047	0.17167	0.00199	2.075	0.047	0.17205	0.00203	2536	48	2578	20	1.6
S	54	52.1	101	78	0.81	-0.044	1.949	0.034	0.18832	0.00128	1.949	0.034	0.18871	0.00130	2670	39	2731	11	2.2
S	3	3.1	323	273	0.87	0.003	1.912	0.024	0.18953	0.00052	1.912	0.024	0.18950	0.00052	2712	28	2738	5	0.9
S	23	22.1	177	77	0.45	0.013	1.716	0.032	0.22658	0.00666	1.716	0.032	0.22646	0.00666	2960	45	3027	47	2.2
M	16	15.1	81	13	0.16	0.486	4.909	0.103	0.07826	0.00116	4.933	0.104	0.07419	0.00194	1190	23	1047	53	-13.7
M	24	23.1	90	30	0.35	0.244	4.959	0.099	0.07739	0.00115	4.971	0.100	0.07534	0.00148	1182	22	1078	39	-9.7
M	46	45.1	83	17	0.21	0.477	4.905	0.089	0.08027	0.00105	4.928	0.090	0.07625	0.00171	1191	20	1102	45	-8.1
M	1	1.1	82	8	0.09	0.421	5.051	0.082	0.08037	0.00093	5.072	0.083	0.07683	0.00146	1160	18	1117	38	-3.9
M	22	21.1	106	34	0.33	0.231	4.813	0.095	0.07928	0.00097	4.824	0.096	0.07734	0.00130	1214	22	1130	34	-7.5
M	55	53.1	46	16	0.36	0.000	4.818	0.106	0.07812	0.00144	4.818	0.106	0.07812	0.00144	1216	25	1150	37	-5.7
M	18	17.1	141	28	0.21	0.136	5.043	0.208	0.07936	0.00083	5.050	0.208	0.07822	0.00101	1165	46	1152	26	-1.1
M	20	19.1	138	29	0.22	0.203	4.756	0.093	0.08045	0.00092	4.766	0.093	0.07874	0.00120	1228	22	1166	30	-5.4
M	5	5.1	89	23	0.26	0.171	5.100	0.083	0.08028	0.00094	5.109	0.083	0.07884	0.00119	1152	18	1168	30	1.4
M	9	8.2	146	7	0.05	0.097	4.908	0.069	0.07983	0.00071	4.912	0.069	0.07901	0.00082	1194	16	1172	20	-1.9
M	43	42.1	267	87	0.34	0.440	5.065	0.073	0.08271	0.00053	5.087	0.074	0.07899	0.00095	1157	16	1172	24	1.3

Table 1. continued

Group ID	Spot no.	Grain. spot	^{238}U (ppm)	^{232}Th (ppm)	$^{232}Th/^{238}U$	f204 (%)	$^{238}U/^{206}Pb$	± 1σ	$^{207}Pb/^{206}Pb$	± 1σ	$^{238}U/^{206}Pb^*$	± 1σ	$^{207}Pb^*/^{206}Pb^*$	± 1σ	$^{238}U/^{206}Pb^*$ date (Ma)	±1σ	$^{207}Pb^*/^{206}Pb^*$ date (Ma)	±1σ	Disc. (%)
M	21	20.1	98	29	0.31	0.045	4.854	0.097	0.07969	0.00096	4.856	0.097	0.07931	0.00103	1207	22	1180	26	-2.3
M	11	10.1	96	29	0.31	0.115	5.007	0.078	0.08031	0.00089	5.013	0.078	0.07934	0.00105	1173	17	1181	26	0.7
M	32	31.1	297	24	0.08	0.054	5.056	0.073	0.07984	0.00052	5.059	0.073	0.07939	0.00057	1163	16	1182	14	1.6
M	26	25.1	542	36	0.07	0.008	4.950	0.088	0.07956	0.00041	4.950	0.088	0.07949	0.00042	1186	19	1184	10	-0.1
M	17	16.1	102	33	0.33	0.187	5.026	0.099	0.08107	0.00098	5.036	0.100	0.07949	0.00126	1168	22	1184	31	1.4
M	12	11.1	56	14	0.26	0.331	4.931	0.090	0.08245	0.00118	4.948	0.091	0.07965	0.00173	1187	20	1188	43	0.1
M	15	14.1	101	16	0.17	0.037	4.914	0.075	0.08002	0.00086	4.916	0.076	0.07971	0.00092	1194	17	1190	23	-0.3
M	6	6.1	100	1	0.01	0.064	5.066	0.076	0.08034	0.00081	5.069	0.076	0.07980	0.00090	1161	16	1192	22	2.6
M	31	30.1	118	42	0.37	0.000	5.095	0.084	0.08015	0.00086	5.095	0.084	0.08015	0.00086	1155	18	1201	21	3.8
M	19	18.1	141	3	0.02	0.034	5.143	0.098	0.08092	0.00085	5.144	0.099	0.08063	0.00090	1145	20	1212	22	5.6
M	60	58.1	103	24	0.24	-0.131	5.034	0.087	0.07960	0.00096	5.027	0.087	0.08071	0.00115	1170	19	1214	28	3.7
M	4	4.1	119	11	0.10	-0.033	5.036	0.076	0.08081	0.00083	5.034	0.076	0.08109	0.00088	1168	16	1224	21	4.5
M	10	9.1	93	3	0.04	-0.158	5.021	0.079	0.08009	0.00091	5.013	0.079	0.08143	0.00113	1173	17	1232	27	4.8
M	62	60.1	56	15	0.28	-0.093	5.259	0.108	0.08134	0.00142	5.254	0.108	0.08213	0.00162	1123	22	1249	39	10.0
M	7	7.1	95	5	0.05	-0.173	5.171	0.244	0.08096	0.00086	5.162	0.244	0.08244	0.00108	1142	52	1256	26	9.1
D	48	46.1	2832	48	0.02	0.009	4.774	0.064	0.08030	0.00018	4.775	0.064	0.08022	0.00018	1226	15	1202	5	-1.9
D	59	57.1	226	82	0.37	0.000	3.907	0.060	0.09971	0.00069	3.907	0.060	0.09971	0.00069	1469	20	1619	13	9.2
D	58	56.1	708	418	0.61	0.027	3.645	0.050	0.10311	0.00038	3.645	0.050	0.10288	0.00039	1563	19	1677	7	6.8
D	29	28.1	128	108	0.87	0.130	3.529	0.056	0.10539	0.00075	3.534	0.056	0.10426	0.00087	1606	23	1701	15	5.6
D	38	37.1	118	32	0.28	0.062	3.500	0.057	0.10591	0.00080	3.502	0.057	0.10537	0.00086	1619	24	1721	15	5.9
D	28	27.1	341	160	0.48	0.007	3.470	0.049	0.10666	0.00045	3.471	0.049	0.10661	0.00046	1632	21	1742	8	6.3
D	69	67.1	109	61	0.58	-0.052	3.543	0.063	0.10686	0.00092	3.541	0.063	0.10731	0.00097	1604	26	1754	17	8.6
D	33	32.1	163	74	0.47	0.049	2.915	0.045	0.13034	0.00076	2.916	0.045	0.12991	0.00079	1901	26	2097	11	9.4
D	68	66.1	1087	196	0.19	0.008	3.493	0.048	0.13282	0.00606	3.493	0.048	0.13274	0.00606	1623	20	2135	80	24.0
D	70	68.1	87	45	0.53	-0.028	2.884	0.053	0.13375	0.00113	2.883	0.053	0.13399	0.00116	1919	31	2151	15	10.8
D	27	26.1	62	29	0.49	0.120	2.797	0.051	0.13959	0.00118	2.801	0.051	0.13852	0.00129	1968	32	2209	16	10.9
D	50	48.1	123	87	0.73	-0.147	2.672	0.054	0.14793	0.00093	2.668	0.053	0.14923	0.00103	2052	36	2337	12	12.2
D	47	19.2	29	21	0.74	-0.202	2.643	0.067	0.14744	0.01531	2.638	0.067	0.14923	0.01531	2072	46	2337	176	11.3
D	66	64.1	194	116	0.62	0.030	2.443	0.038	0.15111	0.00074	2.444	0.038	0.15085	0.00075	2211	30	2356	9	6.1
D	61	59.1	257	119	0.48	0.016	2.564	0.039	0.15268	0.00067	2.565	0.039	0.15254	0.00067	2122	28	2375	8	10.6
D	57	55.1	193	129	0.69	0.052	2.533	0.040	0.15367	0.00561	2.534	0.040	0.15321	0.00562	2144	29	2382	62	10.0
D	65	63.1	361	203	0.58	-0.011	2.419	0.035	0.15403	0.00275	2.419	0.035	0.15413	0.00275	2231	28	2392	30	6.8
D	25	24.1	68	78	1.18	-0.099	2.055	0.044	0.15520	0.00116	2.053	0.044	0.15608	0.00124	2558	46	2414	13	-6.0
D	52	50.1	258	143	0.57	0.015	2.321	0.035	0.16078	0.00067	2.321	0.035	0.16065	0.00068	2309	30	2463	7	6.2
D	35	34.1	761	66	0.09	0.000	2.861	0.039	0.16411	0.00517	2.861	0.039	0.16411	0.00517	1932	23	2498	53	22.7
D	72	70.1	223	144	0.67	-0.017	2.649	0.040	0.16763	0.00076	2.648	0.040	0.16778	0.00077	2065	27	2536	8	18.6
D	14	13.1	167	84	0.52	-0.025	1.849	0.026	0.22975	0.00082	1.849	0.026	0.22997	0.00083	2787	32	3052	6	8.7

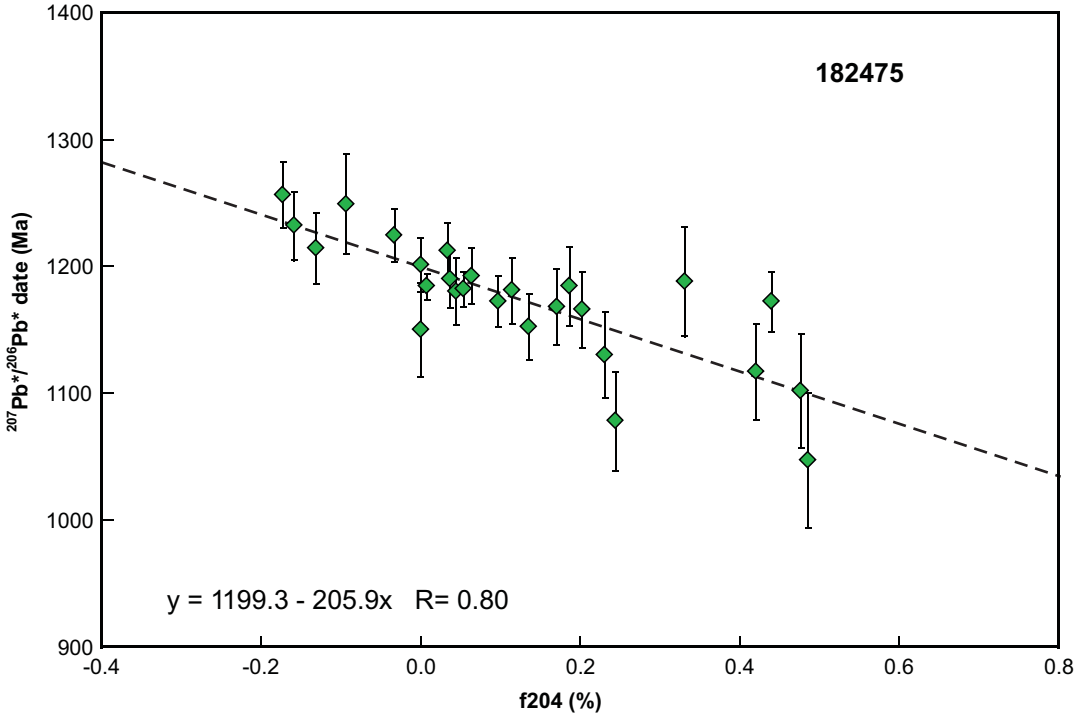

Figure 3. Correlation between ^{207}Pb*/^{206}Pb* date (corrected for common Pb using measured ^{204}Pb) and *f*204, for analyses of zircon rims in sample 182475: migmatitic gneiss, Big Red prospect. The dashed line indicates a regression through data in Group M; the equation of the best-fit line is also shown. R is Pearson's correlation coefficient.

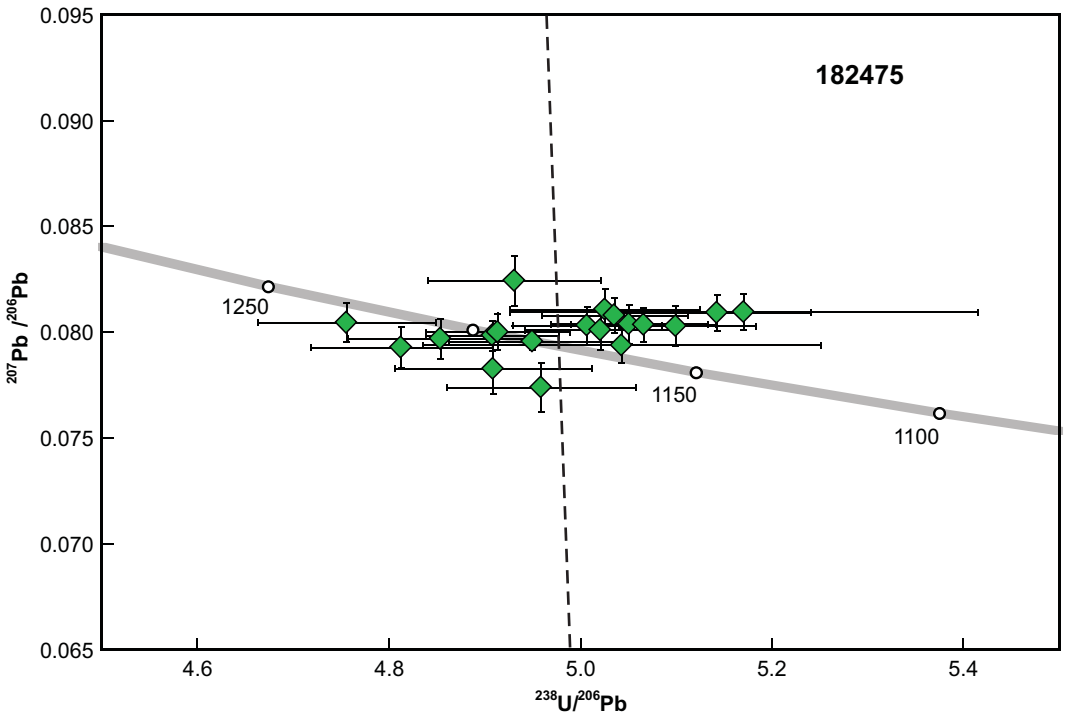

Figure 4. Expanded view of U–Pb analytical data, not corrected for common Pb, for Group M, from sample 182475: migmatitic gneiss, Big Red prospect. Symbols as in Figure 2. The dashed line indicates a regression from initial Pb.

on 20–22 October, using SHRIMP B. Analyses 1.1 to 14.1 (spot numbers 1–15) were obtained during the first session, together with nine analyses of the BR266 standard, of which seven analyses indicated an external spot-to-spot (reproducibility) uncertainty of 0.99% (1σ) and a $^{238}U/^{206}Pb^*$ calibration uncertainty of 0.39% (1σ). Analyses 15.1 to 25.1 (spot numbers 16–26) were obtained during the second session, together with eight analyses of the BR266 standard, of which seven analyses indicated an external spot-to-spot (reproducibility) uncertainty of 1.61% (1σ) and a $^{238}U/^{206}Pb^*$ calibration uncertainty of 0.60% (1σ). Analyses 26.1 to 70.1 (spot numbers 27–72) were obtained during the third session, together with 21 analyses of the BR266 standard, of which 17 analyses indicated an external spot-to-spot (reproducibility) uncertainty of 1.25% (1σ) and a $^{238}U/^{206}Pb^*$ calibration uncertainty of 0.32% (1σ). Calibration uncertainties are included in the errors of $^{238}U/^{206}Pb^*$ ratios and dates listed in Table 1. Common-Pb corrections were applied to all analyses using contemporaneous isotopic compositions determined according to the model of Stacey and Kramers (1975).

Results

Seventy-two analyses were obtained from 70 zircons. Results are listed in Table 1, and shown in a concordia diagram (Figs 2 and 4), an X–Y correlation plot (Fig. 3), and a probability density diagram (Fig. 5).

Interpretation

The analyses are concordant to moderately discordant (Fig. 2). Twenty-one analyses >1300 Ma are >5% discordant (Group D), and one analysis is interpreted as a mixture of core and rim material. The dates obtained from these 22 analyses (Group D; Table 1) are imprecise or unreliable, and are considered not to be geologically significant. The remaining 50 analyses can be divided into three groups, based on their positions within the crystals and $^{207}Pb^*/^{206}Pb^*$ or $^{238}U/^{206}Pb$ ratios. In the <1200 Ma population, $^{207}Pb^*/^{206}Pb^*$ dates correlate with their common-Pb contents (f204, Fig. 3), indicating that corrections using ^{204}Pb are inaccurate for some or all of these analyses. The date for zircon rims in this sample is therefore determined from the intersection of a regression through uncorrected data with the concordia curve (Fig. 4), anchored at contemporaneous initial Pb ($^{207}Pb/^{206}Pb$ = 0.9240 at 1180 Ma; Stacey and Kramers, 1975).

Group Y comprises one analysis of a zircon core (Table 1), which yields a $^{207}Pb^*/^{206}Pb^*$ date of 1685 ± 11 Ma (1σ).

Group S comprises 23 analyses of 23 zircon cores (Table 1), which yield $^{207}Pb^*/^{206}Pb^*$ dates of 3027–1741 Ma.

Group M comprises 26 analyses of 26 zircon rims (Table 1), for which the regression intersects the concordia curve at 1176 ± 10 Ma (MSWD = 1.5).

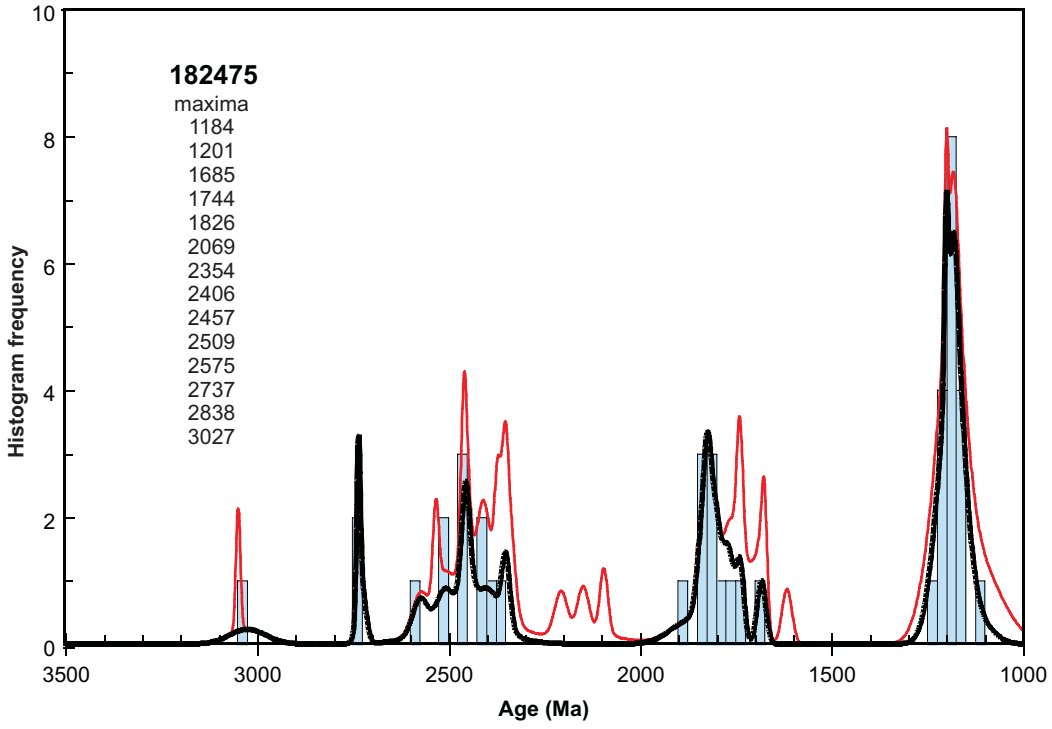

Figure 5. Probability density diagram and histogram for sample 182475: migmatitic gneiss, Big Red prospect. Thick curve, maxima values, and frequency histogram (bin width 25 Ma) include only accepted data (50 analyses of 50 zircons). Thin curve includes all data (72 analyses of 70 zircons).

It is possible that all of the analyses in Groups Y and S are of unmodified detrital zircons, in which case the date of 1685 ± 11 Ma (1σ) for the single analysis in Group Y represents a maximum depositional age for the sedimentary precursor. A more conservative estimate of the maximum depositional age can be based on the weighted mean $^{207}Pb^*/^{206}Pb^*$ date of 1773 ± 20 Ma (MSWD = 0.5) for two analyses (12.1, 29.1; Table 1) in Group S.

The data for combined Groups Y and S indicate significant age components at c. 1826 and c. 2457 Ma, and several minor components in the range 3027–1685 Ma. These are interpreted as the ages of zircon-crystallizing rocks in the detrital source region(s), or as the ages of detrital components within sediments that have been reworked. These age components are consistent with this paragneiss belonging to either the Paleoproterozoic Barren Basin or the Mesoproterozoic Arid Basin (Spaggiari et al., 2011).

The date of 1176 ± 10 Ma for the 26 zircon rim analyses in Group M is interpreted as the age of a high-grade metamorphic and migmatization event during Stage II (1215–1140 Ma) of the Albany–Fraser Orogeny (Clark et al., 2000).

References

Clark, DJ, Hensen, BJ and Kinny, PD 2000, Geochronological constraints for a two-stage history of the Albany–Fraser Orogen, Western Australia: Precambrian Research, v. 102, no. 3, p. 155–183.

Kirkland, CL, Wingate, MTD and Spaggiari, CV 2012a, 182473: migmatitic gneiss, Big Red prospect; Geochronology Record 1050: Geological Survey of Western Australia, 6p.

Kirkland, CL, Wingate, MTD and Spaggiari, CV 2012b, 182474: granite vein, Big Red prospect; Geochronology Record 1051: Geological Survey of Western Australia, 4p.

Kirkland, CL, Wingate, MTD and Spaggiari, CV 2012c, 182476: migmatitic gneiss, Big Red prospect; Geochronology Record 1053: Geological Survey of Western Australia, 4p.

Kirkland, CL, Wingate, MTD and Spaggiari, CV 2012d, 182477: mafic granulite, Big Red prospect; Geochronology Record 1055: Geological Survey of Western Australia, 4p.

Nelson, DR, Myers, JS and Nutman, AP 1995, Chronology and evolution of the Middle Proterozoic Albany–Fraser Orogen, Western Australia: Australian Journal of Earth Sciences, v. 42, p. 481–495, DOI:10.1080/08120099508728218.

Spaggiari, CV, Kirkland, CL, Pawley, MJ, Smithies, RH, Wingate, MTD, Doyle, MG, Blenkinsop, TG, Clark, C, Oorschot, CW, Fox, LJ and Savage, J 2011, The geology of the east Albany–Fraser Orogen — a field guide: Geological Survey of Western Australia, Record 2011/23, 98p.

Stacey, JS and Kramers, JD 1975, Approximation of terrestrial lead isotope evolution by a two-stage model: Earth and Planetary Science Letters, v. 26, p. 207–221.

Tillick, D 2010, Final report of co-funded government–industry drilling program at the Eucla Project, E28/1608, September 2010; Teck Australia Pty Ltd: Geological Survey of Western Australia, Statutory mineral exploration report, A88011, 23p. (unpublished).

Recommended reference for this publication

Kirkland, CL, Wingate, MTD and Spaggiari, CV 2012, 182475: migmatitic gneiss, Big Red prospect; Geochronology Record 1052: Geological Survey of Western Australia, 7p.

Data obtained: 22 October 2011

Data released: 30 June 2012